JOURNAL OF MATERIALS SCIENCE 28 (1993) 3149–3154

Shear strength resulting from static friction of some thermoplastics

S. H. BENABDALLAH
Department of Mechanical Engineering Royal Military College of Canada, Kingston, Ontario, Canada K7K 5LO

The effects of normal load and roughness on the static shear strength of three thermoplastics have been investigated for the case of contact between a plastic sample and a very smooth metallic plate. An apparatus which provides a gradual increase in the tangential load was used to measure the minimum force required to shear the adhesion between the two surfaces when subjected to a normal load. This force was set equal to the adhesion component of friction F_f. The real area of contact A_r was also measured using an optical device designed to handle samples and experimental conditions similar to the friction tests. This permitted the evaluation of static shear strength τ as the ratio F_f/A_r. The experimental results for ultra-high molecular weight polyethylene (UHMWPE) show that the relationship between τ and the real contact pressure P can be represented by a regression function of order three. For this material, there is a decrease of τ when the asperities undergo elastic deformations. However, an increase in τ is found when plastic deformation of the asperities occurs. This transition was noted at the region where P is equal to the yield strength S_y of the material. The acetal Delrin also showed a decrease of τ when $P < S_y$ and, although it could not be verified experimentally, it is assumed that it would behave in the same manner as the previous material for higher P. A strong dependence of τ on the initial roughness of the contacting surface was observed for both materials. The results obtained with nylon (PA 66) show an increase of τ with P, even when P is lower than S_y. This difference in behaviour compared to the previous materials is related to the brittleness of the asperities which is a result of its relatively low glass transition temperature. No effect of the roughness on the shear strength was found for this material. The relationship between τ and P can be very well approximated by linear functions whose parameters depend on the type of deformation that occurs at the interface. These parameters are derived and reported.

Nomenclature

A_a	Apparent area of contact
A_r	Real area of contact
b	Semi-contact length
c.l.a.	Centre-line average
d_i	Section width of an asperity at a distance h_i from the crest
E	Young's modulus
E'	Given by $1/E' = [(1 - \nu_1^2)/E_1] + [(1 - \nu_2^2)/E_2]$
F	Concentrated load
F_f	Adhesion component of friction
H	Hardness
h_i	Distance from the crest of an asperity
L	Length along which the contact is made
N	Total number of peaks
n	Number of asperities making contact
P	Real contact pressure
R	Mean radius of curvature of asperity tips
S_y	Yield strength
α	Constant
δ_v, δ_h	Vertical and horizontal magnification, respectively
ν	Poisson's ratio
σ	Standard deviation
τ	Shear strength
τ_0	Constant

1. Introduction

When solids are brought together, contact is made over the real (as opposed to the apparent) area of contact. Adhesion occurs as a result of this contact and of the frictional resistance to sliding which arises from the shearing of cold-welded junctions which have formed at the contact. Previous studies have investigated the shear strength of polymeric materials during friction; however, unlike the present study, polymers were deposited as thin films on hard, smooth substrates followed by the sliding of the films over one another [1]. A complete review of this subject has been done by Towle [2].

If the shear strength of the junctions which form the real area of contact A_r is τ, then the frictional force can

0022–2461

be written as

$$F_f = A_r\tau \quad (1)$$

To determine the shear strength the real area of contact and the frictional force should be measured experimentally. Many techniques of measuring friction are available but the measurement of A_r is rather complicated.

To overcome the difficulty of measuring A_r many authors have used samples with particular geometries allowing a theoretical evaluation using classical theories of contact such as Hertz's theory, or assumed that A_r supporting the load is determined solely by the yield strength or the indentation hardness of the solid.

A relationship between τ at the interface and the real contact pressure P has been derived [3]:

$$\tau = \tau_0 + \alpha P \quad (2)$$

Where τ_0 and α are constants.

Some authors have approximated τ to the value of the bulk shear strength of the softer material. Current published papers deal with the shear strength resulting from dynamic friction. In order to avoid the influence of work-hardening of the plastic material and of the temperature rise generated by the energy dissipated by dynamic friction, we consider in the present work the static shear strength.

In this paper, an attempt has been made to consider the minimum tangential force which would shear the adhesive junctions at areas of intimate contact between bulk plastic samples and a metallic plate brought into contact by a normal load. The plastic–metal contact has been chosen because of its practical applications. The real area of contact was also measured. This has permitted investigation of the effects of contact pressure and roughness on the static shear strength when three engineering thermoplastics are tested.

2. Experimental procedure

2.1. Measurement of the adhesion force

The design of apparatus used in this study has been described in greater detail elsewhere [4]. It is based on the principle of the slide angle tester which provides a gradual increase of the tangential load that breaks the adhesion at the interface of two components making contact. With this sled apparatus the precise instant of transition from the state of rest to that of relative movement can be detected, and the direct manifestation of adhesion during tangential separation may be considered.

2.2. Measurement of the real area of contact

An optical device was developed to measure A_r. It is based on the perturbation of total internal reflection of a light beam in the region of contact between a glass prism and a machined polymeric surface. The design concepts have been outlined in a previous paper [5]. It should be emphasized that this device considers the contact between a glass prism and the plastic sample. In this study, the two types of contact (plastic–metal and plastic–glass) are considered to be similar because the hardness and rigidity of metal and glass are very high compared to plastic materials. Furthermore, the metallic plate is machined and polished to ensure a similar surface finish. Finally, similar plastic samples and identical loading conditions were used for both types of experiment. Therefore we will consider the real area of contact developed during the adhesion tests as being equal to the one measured under the same conditions.

2.3. Topographical parameters of contacting surfaces

Measurements and calculations of the topographical parameters are necessary for the theoretical calculation of A_r in order to compare it with the measured values. The signals emitted by a profilometer (Clevite Brush-Surfindicator) were fed into a data acquisition system.

The attenuation rate limits beyond the passband of the long-wavelength end were produced by two idealized R–C networks. A standard cut-off of 0.8 mm was considered. The maximum digitizing rate of 2000 Hz, used with a stylus traverse speed of 0.3175 mm s^{-1}, gave a maximum ordinate separation of 0.16 μm. About 78 400 ordinates were recorded for a single trace. The resolution for electronic treatment is estimated at 0.02 μm in the vertical direction and 0.09 μm along the horizontal. A program written in Basic yielded the following information from the digitized profile of the surface: roughness represented by the c.l.a. (centre-line average), total number of peaks N, mean radius of curvature of asperity tips R, and standard deviation of asperity height σ. The curvature radii were determined using the following equations [6]:

$$R_i = \frac{\delta_v}{\delta_h^2}\left(\frac{d_i^2}{8\,h_i}\right) \quad (3)$$

where δ_v and δ_h are the vertical and horizontal magnifications. The section width of d_i is found at a distance h_i from the crest equal to 0.3 c.l.a.

The value reported is the mean radius calculated using the following equation:

$$R = \frac{1}{n}\sum R_i \quad (4)$$

The transverse radius is infinity because the crest of each peak is assimilated to a cylinder making contact with a flat and very smooth surface of hard material (glass).

The values of the topographical parameters for the plastic materials considered in this study are reported in Table I. The surface roughness for a metallic plate made of cold-rolled steel, AISI 4340, and a glass prism was about 0.1 μm c.l.a.

2.4. Properties of materials and experimental conditions

Ultra-high molecular weight polyethylene (UHMWPE, Hercules 1900 supplied by Solidur Plastics),

TABLE I Topographical parameters of plastic samples tested

Material	c.l.a. (μm)	Number of peaks, N	Standard deviation, σ (μm)	Mean radius of curvature of the asperity tips, R (μm)
UHMWPE	3.2	34725	4.6	33
	17.3	12031	19.8	21
	34.3	3147	38.5	38
PA 66	3.7	33997	4.9	22
	17.9	13097	20.7	20
	39.7	3631	40.5	48
POM	3.0	34640	3.9	20
	17.2	12252	19	15
	33.5	3418	36.5	26

TABLE II Mechanical properties of plastics and glass used in this study

Property	Norm used for evaluation	UHMWPE	PA 66	POM	Glass
Micro-indentation hardness, H (MPa)	Vickers	73.2	204.3	130.5	–
Elastic modulus, E (GPa)	ASTM D-638	1.21	2.53	2.21	73[a]
Poisson's ratio	Calculated from tensile and shear moduli	0.46[b]	0.34[b]	0.35[b]	0.22[a]
Bulk shear strength (MPa)	ASTM D-732	20.4	70	61.5	–
Yield strength S_y (MPa)	ASTM D-638	19	67	69.2	–

[a] From [7].
[b] From [8].

polyamide 66 (PA 66, Zytel 101, DuPont) and polyoxymethylene (POM, Delrin 500, DuPont) were considered in this study. Small blocks of these plastics with an apparent area of contact 1 cm × 2 cm, $A_a = 2\ cm^2$ were used as samples. They were cut from extruded sheets and the contacting surface machined in order to produce a uniform roughness.

Experiments were conducted under unlubricated conditions with a range of normal load, 5 to 200 N (which gives a range of apparent contact pressure, 25×10^{-3} to 1 MPa) at room temperature. A new sample was used for each unvarying condition (normal load and roughness). The parameters measured and recorded were the tangential force necessary to overcome adhesion and the real area of contact as functions of normal load and roughness. All series of tests were repeated several times to ensure consistency of results, so that each plot represents an average of the data of five identical tests.

Some of the mechanical properties of the materials considered in this study, and necessary for the following calculations, are presented in Table II. These properties were either measured or taken from engineering handbooks.

3. Results and discussion

3.1. The real area of contact

An attempt is made here to compare the measured real area of contact with predicted values, using two theoretical models based on Hertz's theory and the theory of elastic contact proposed by Greenwood and Williamson (GW) [9].

The machining of the contacting surface of the plastic samples was performed in such a manner that asperities with cylindrical tips of length $L = 1$ cm (width of sample) were produced. Therefore, to theoretically evaluate A_r, we considered the analytical solution to the Hertz problem, when two cylinders are brought into contact. Based on this theory, Chandrasekaran *et al.* [10] derived the following equation to evaluate the semi-contact length b, when one contacting body is flat:

$$b = 1.13\left[\frac{F}{nL}\left(\frac{R}{E'}\right)\right]^{1/2} \tag{5}$$

where

$$\frac{1}{E'} = \frac{1-\nu_1^2}{E_1} + \frac{1-\nu_2^2}{E_2} \tag{6}$$

F is a concentrated load applied at the centre of the sample, n the total number of asperities in contact, E_1 and E_2 the Young's moduli of the glass (prism) and the plastic material (sample), and ν_1 and ν_2 their respective Poisson's ratios.

On the other hand, Bhushan [11] has developed general and simplified equations based on GW analysis carried out for metals to find, among other things, the number of asperities in contact, and the total real area of contact for plastic materials making contact with a smooth and rigid surface. Assuming an elastic contact, the number of contact spots is determined by

$$\frac{n}{N} = 1.21\left(\frac{F}{N R^{1/2}\,\sigma^{3/2}\,E'}\right)^{0.88} \tag{7}$$

Knowing n, the real contact area can be calculated as

$$A_r = nbL \tag{8}$$

The second model considered for the evaluation of A_r [11] is

$$\frac{A_r}{A_a} = 2.4\,\frac{N R \sigma}{A_a}\left(\frac{F}{N R^{1/2}\,\sigma^{3/2}\,E'}\right)^{0.44} \tag{9}$$

It should be noted that to obtain Equations 7 and 9, a transformation had been made to the original equations reported by Bhushan. In fact the density of asperities η was replaced by the ratio N/A_a. Also it was verified that in the case of the present study the value of $(N\ R\ \sigma/A_a)$ is about 0.03 for all the specimens tested, which agrees with the results obtained by Archard [12].

Because of the viscoelastic behaviour of the plastics, all the experimental results of the measurement of the real contact area were taken about 130 s after the loading time. This allows for the steady state to be reached.

Some of the experimental results are plotted in Figs 1, 2 and 3. The material tested and its corresponding roughness are shown on each figure. The ordinate is the bearing area ratio of the real contact area to the nominal contact area, and the abscissa is the dimensionless load F/A_aH. These points follow a power law which was established through a least-squares fit represented on the figures by solid lines. These lines were constrained to take the form $A_r/A_a = \beta(F/A_aH)^m$ in which the value of the exponent m depends on the type of plastic material. The proportionality constant β depends on the roughness of the contacting plastic surface. Table III lists the values of m and β for the conditions of this study.

Comparison of experimental results made with the predicting values obtained using Equations 8 and 9 is shown in Figs 1 to 3. Figs 1 and 3 show also the results when the real area of contact is evaluated from the ratio of the load and the hardness of the material.

The experimental results are reasonably consistent with the Hertz theory; however, the model of Bhushan seems to underestimate the real contact area when the roughness of the plastic sample increases. It is clear that the explanation of these deviations is not the main object of this study, but it is necessary to show that the measured data are comparable with those predicted by two theoretical models.

3.2. The adhesion force

In this study it was assumed that the measured tangential force which tends to shear the adhesion at the interface represents the static friction force. Thus the deformation (ploughing) component of friction will not be considered due to the smoothness of the metallic surface.

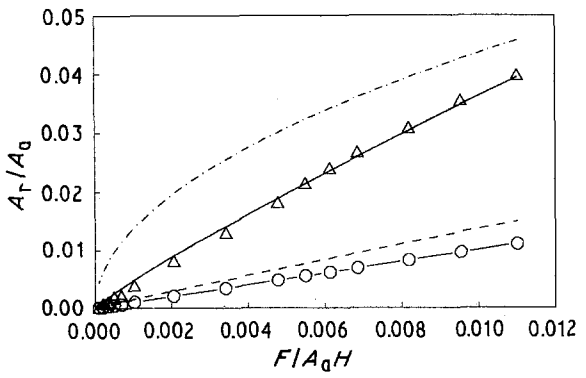

Figure 1 △ Bearing area ratio versus dimensionless load: case of UHMWPE and surface roughness c.l.a. = 3.2 μm. Theoretical predictions: (—○—) Hertz (Equation 8), (— — —) Bhushan (Equation 9). (○) evaluation of A_r from F/H.

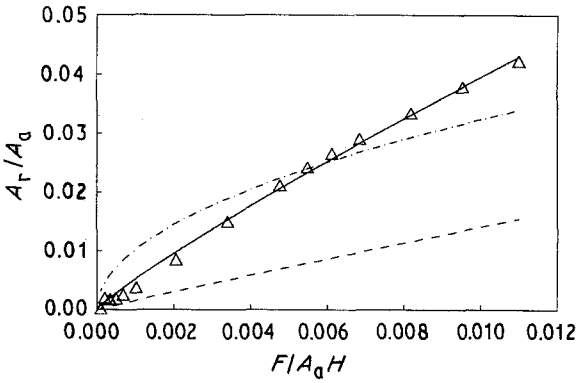

Figure 2 (△) Bearing area ratio versus dimensionless load: case of UHMWPE and surface roughness c.l.a. = 17.3 μm. Theoretical predictions: (—○—) Hertz (Equation 8), (— — —) Bhushan (Equation 9).

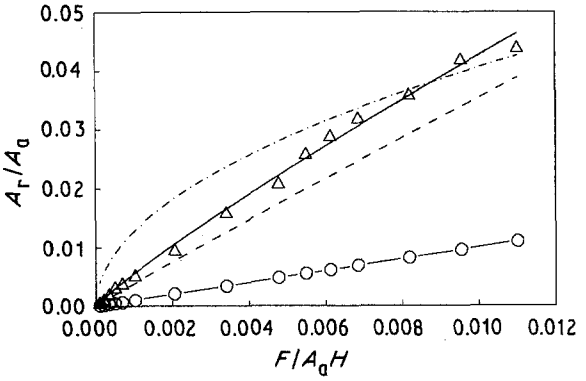

Figure 3 △ Bearing area ratio versus dimensionless load: case of UHMWPE and surface roughness c.l.a. = 34.3 μm. Theoretical predictions: (—○—) Hertz (Equation 8), (— — —) Bhushan (Equation 9). (○) evaluation of A_r from F/H.

TABLE III Experimental values of m and β in $A_r/A_a = \beta(F/A_aH)^m$

Variable	c.l.a. (μm)	UHMWPE	PA 66	POM
m		0.88	0.84	0.96
β	~ 3	2.45	2.34	3.2
	~ 18	2.27	2.02	2.7
	~ 35	2.08	1.79	2.53

Fig. 4 shows an example of the variation of the static friction force as a function of dimensionless load. A power law with a negative exponent, representing the variation of the static friction as a function of the normal load, has been found for each material considered in this study. This suggests that the static coefficient of friction is not a constant of the material but decreases with the normal load. We should point out that for plastic materials the decrease of the dynamic coefficient of friction when the normal load increases has already been observed by many authors.

3.3. The shear strength

The observed shear strength of UHMWPE is shown in Figs 5 and 6 as a function of the real contact

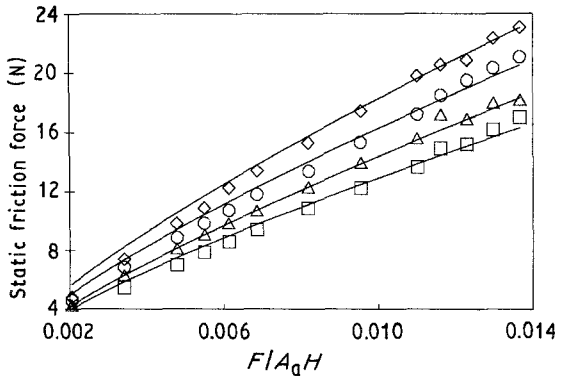

Figure 4 Static friction force versus dimensionless load for UHMWPE; surface roughness c.l.a. = (◇) 0.85, (○) 3.2, (△) 17.3 and (□) 34.3 μm.

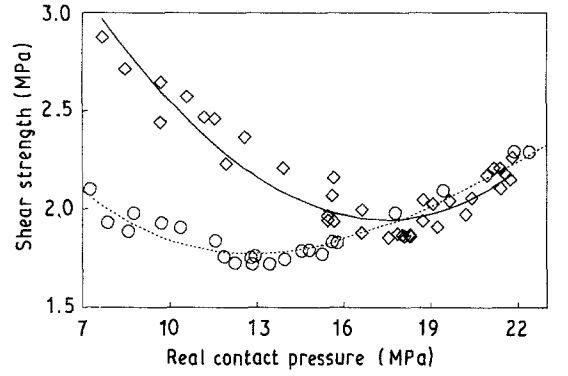

Figure 5 Shear strength versus real contact pressure for UHMWPE; surface roughness c.l.a. = (○) 0.85 and (◇) 3.2 μm.

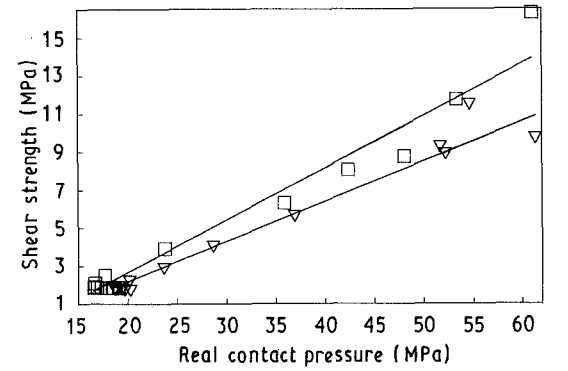

Figure 6 Shear strength versus real contact pressure for UHMWPE; surface roughness c.l.a. = (□) 17.3 and (▽) 34.3 μm.

pressure for four different roughnesses of the plastic sample. According to these figures, data in the range of the contact pressure considered show that the relationship between the two parameters is well represented by a regression of order three (lines on the figures).

Fig. 5 shows three distinctive regions. The first region is the decrease of τ with the real contact pressure P, where the significant decrease of the static coefficient of friction may play an important role. The second region is a transition zone. The third zone is characterized by an increase of τ which could be due to the increase of A_r. It should be noted that at high contact pressure the friction coefficient will asymptotically approach a small value.

When samples with rough contacting surface were tested, only two regions are present as shown in Fig. 6. In this case, due to the very small real area of contact, even light loads have generated high contact pressures. There is an apparent break in the data near 19 MPa which suggests the transition from elastic to plastic deformation of the asperities due to loading, since the yield stress of this material is $S_y = 19$ MPa (reported in Table II).

The combination of the results presented in Figs 5 and 6 leads to the conclusion that τ decreases slightly with load when the asperities are deformed elastically. τ remains constant at the regions of transition to plastic deformations followed by an increase.

Fig. 7 shows the same data as Figs 5 and 6 but plotted over a limited range of pressure, higher than S_y. Accordingly, it is sufficient to retain only the first two terms of the regression and consider a linear relationship between τ and P, which agrees with Equation 2. The least-squares fit of data in that pressure range to straight lines yielded the parameters reported in Table IV.

These experimental results indicate that the initial roughness of the contacting surface of the plastic sample plays a significant role in determining the static shear strength. A more consistent conclusion cannot be drawn at this stage, since there is no obvious relationship between the two parameters when P is higher than S_y.

Fig. 8 shows the experimental results for POM, at the first stage where $P < S_y$. In this case the experi-

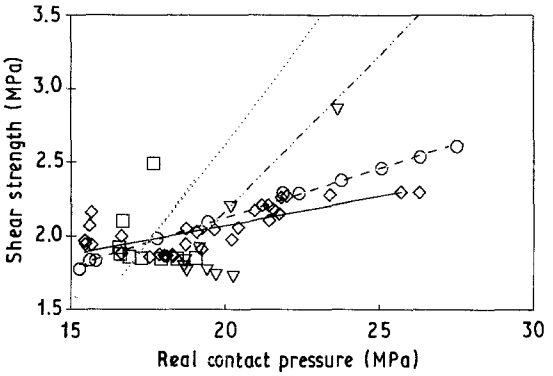

Figure 7 Shear strength versus real contact pressure for UHMWPE; surface roughness c.l.a. = (○) 0.85, (◇) 3.2, (□) 17.3 and (▽) 34.3 μm.

TABLE IV Values of parameters of the least-squares fit of shear strength constrained to take the form $\tau = \tau_0 + \alpha P$, where $P > S_y$ for UHMWPE and $P < S_y$ for POM and PA 66

c.l.a. (μm)	UHMWPE τ_0 (MPa)	UHMWPE α	POM τ_0 (MPa)	POM α	PA 66 τ_0 (MPa)	PA 66 α
~ 0.8	0.805	0.07	–	–	1.931	0.297
~ 4	0.496	0.07	12.42	– 0.16		
~ 17	– 2.9	0.277	14.31	– 0.16		
~ 40	– 2.153	0.214	15.88	– 0.16		

τ_0 is negative in two cases. Therefore, τ_0 is a curve-fitting parameter rather than the value of shear strength when $P = 0$.

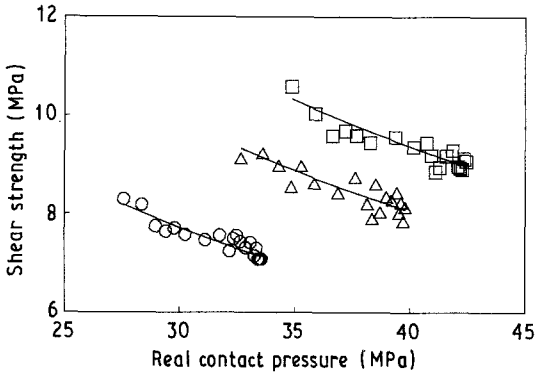

Figure 8 Shear strength versus real contact pressure for POM; surface roughness c.l.a. = (○) 3.0, (△) 17.2 and (□) 33.5 μm.

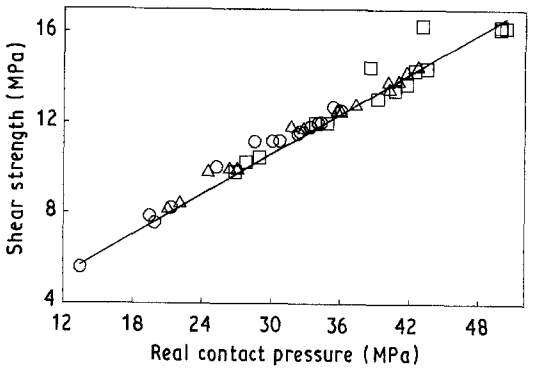

Figure 9 Shear strength versus real contact pressure for PA 66, surface roughness c.l.a. = (○) 3.7, (△) 17.9 and (□) 39.7 μm.

mental device for measuring the real area of contact, especially the loading system, did not allow experiments to be conducted at pressures higher than S_y. It can be expected that this material behaves in the same way as UHMWPE. Therefore τ should start increasing when $P > S_y$. A least-squares fit of data was also performed and gave the parameters reported in Table IV.

All the observations cannot be generalized since PA 66 behaves in a different manner, as shown in Fig. 9. This figure shows an increase of τ with P. Also in the PA 66 study, the roughness does not play a significant role. The parameters of the straight line obtained by a least-squares fit are shown in Table IV. The difference in behaviour of PA 66 as compared to the two other materials is due to its relatively high glass transition temperature, which leads to brittle asperities of the contacting surface.

It is also shown that the static shear strength cannot be accurately approximated to the bulk shear strength and is strongly dependent on the normal load.

4. Conclusion

In this study the effect of normal load and roughness on the static shear strength at the surface of contact of a plastic sample and a metallic plate when a tangential force is acting in order to break the adhesion between the two materials has been investigated. A specially designed apparatus was used to provide a gradual increase of the tangential load until relative movement is detected. This force was then set equal to the adhesion component of friction which is theoretically equal to the product of τ and A_r. A_r was measured using an optical device designed to handle similar samples and experimental conditions as the friction tests. Three engineering thermoplastics, UHMWPE, POM and PA 66, have been considered.

The experimental results for UHMWPE have shown that the relation between τ and the real contact pressure P is represented by a regression of order three. Three stages have been identified. There is a decrease of τ when the asperities deform elastically, a transition where τ remains almost constant when P approaches the same value as the yield stress of the material, and an increase of τ when the asperities deform plastically.

POM has also shown a decrease of τ when $P < S_y$, and it can be assumed that it behaves in the same manner as UHMWPE. For both materials there is a strong dependence of τ on the initial roughness of the contacting surface.

The results obtained with PA 66 show an increase of τ with P, even when P is lower than S_y. This difference in behaviour could be related to the brittleness of the asperities due to its relatively low glass transition temperature. No effect of the roughness on the shear strength has been found for this material.

It has been stated by some authors who have determined the shear behaviour of polymers as thin films, that the relationship between τ and P can be very well approximated by linear functions. The parameters of these functions depend on the type of deformation that occur at the interface.

The shear strength cannot be reasonably approximated to its bulk value in the case of the plastic materials tested.

References

1. B. J. BRISCOE and D. TABOR, *Wear* **34** (1975) 29.
2. L. C. TOWLE, in "Advances in Polymer Friction and Wear", edited by L. H. Lee (Plenum, New York, 1974) p. 179.
3. J. K. AMUZU, B. BRISCOE and D. TABOR, *ASLE Trans.* **20** (1977) 354.
4. S. H. BENABDALLAH and H. YELLE, *J. Mater. Sci.* **26** (1991) 2445.
5. S. H. BENABDALLAH and J. LAPIERRE, *J. Mater. Sci.* **25** (1990) 3497.
6. I. V. KRAGELSKI and V. V. ALISIN, "Friction, Wear, Lubrication", Vol. 1 (Pergamon, New York, 1981) p. 24.
7. G. W. McLELLAN and E. B. SHAND, "Glass Engineering Handbook" (McGraw-Hill, New York, 1984) p. 136.
8. "Modern Plastics Encyclopedia" 57, Vol. 10A (McGraw-Hill, New York, 1980) p. 595.
9. J. A. GREENWOOD and J. B. P. WILLIAMSON, *Proc. R. Soc. London* **A295** (1966) 300.
10. N. CHANDRASEKARAN, W. E. HAISLER and R. E. GOFORTH, *Finite Elem. Anal. Design* **3** (1987) 39.
11. B. BHUSHAN, *J. Tribol., Trans. ASME* **106** (1984) 26
12. J. F. ARCHARD, *Tribol. Internat.* **7** (1974) 213.

Received 9 July 1991
and accepted 17 November 1992